Phytochemistry 230 (2025) 114315

Contents lists available at ScienceDirect

Phytochemistry

journal homepage: www.elsevier.com/locate/phytochem

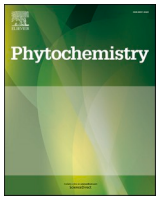

Thuwalamides A–E: Polychlorinated amides from the marine sponge *Lamellodysidea herbacea* collected from the Saudi Arabian Red Sea

Mohamed A. Tammam [a,b], Nikolaos Tsoureas [c], Dafni-Ioanna Diakaki [a], Carlos M. Duarte [d], Vassilios Roussis [a], Efstathia Ioannou [a,*]

[a] Section of Pharmacognosy and Chemistry of Natural Products, Department of Pharmacy, National and Kapodistrian University of Athens, Panepistimiopolis Zografou, Athens, 15771, Greece
[b] Department of Biochemistry, Faculty of Agriculture, Fayoum University, Fayoum, 63514, Egypt
[c] Laboratory of Inorganic Chemistry, Department of Chemistry, National and Kapodistrian University of Athens, Panepistimiopolis Zografou, Athens, 15784, Greece
[d] Marine Science Program, Division of Biological and Environmental Sciences and Engineering, King Abdullah University of Science and Technology, Thuwal, 23955-6900, Saudi Arabia

ARTICLE INFO

Keywords:
Lamellodysidea herbacea
Dysideidae
Sponge
Red sea
Thuwalamides a–e
Polychlorinated amides
Antibacterial activity

ABSTRACT

Thuwalamides A–E (**1**, **3**, **5**, **6** and **8**), previously undescribed polychlorinated amides, along with ten previously reported related compounds (**2**, **4**, **7** and **9**–**15**), were isolated from the organic extract of the marine sponge *Lamellodysidea herbacea* (Keller), collected off the village of Thuwal in the Red Sea at Saudi Arabia. The structures of the isolated compounds have been determined through extensive analysis of their NMR and MS data, while their absolute stereochemistry was unequivocally established via single crystal X-ray diffraction. Additionally, the absolute stereochemistry of the previously reported compounds **2** and **4**, whose configuration was not determined, has also been established using single-crystal X-ray crystallographic analysis. The antibacterial activity of compounds **1**–**15** was evaluated against *Escherichia coli* and *Staphylococcus aureus*. Among them, compound **14** displayed activity against *S. aureus* comparable to vancomycin that was used as a positive control with a MIC value of 4 μg/mL.

1. Introduction

Marine sponges (Porifera) rank amongst the most prolific sources of bioactive natural products, yielding up to now approximately 30% of all marine natural products (MarinLit, 2024). Sponges are sessile invertebrates lacking an innate immune system or physical defensive structures and therefore rely heavily for their protection on the bioactive molecules they or their symbionts produce (Hong et al., 2022). Compounds isolated from sponges include mostly alkaloids, peptides, terpenoids, steroids and macrolides, exhibiting a wide spectrum of bioactivities, such as anticancer, anti-inflammatory, antibacterial, antifungal, antimalarial, analgesic, immunomodulatory, and neuroprotective activities (Carroll et al., 2024; MarinLit, 2024). It is worth noting that the medicinal uses of sponges can be traced back to the Alexandrian physicians, as described by the Roman historian Plinius (Sipkema et al., 2005).

The sponge genus *Lamellodysidea* Cook & Bergquist (Dysideidae), which resulted from the splitting of the genus *Dysidea*, currently includes two species, i.e. *Lamellodysidea herbacea* (Keller) and *L. chlorea* (de Laubenfels) (Sauleau and Bourguet-Kondracki, 2005; de Voogd et al., 2024). Up to now, several compounds, including furanosesquiterpenes, polybrominated diphenyl ethers, chlorinated diketopiperazines, polychlorinated amides and diterpenes, with various biological activities have been reported from species of the genera *Dysidea* and *Lamellodysidea* (Fathallah et al., 2023; MarinLit, 2024).

The Red Sea, characterized by unique biotic and abiotic conditions, relatively high temperature and relatively young geologic age, exhibits an enormous biodiversity. Nonetheless, its marine biodiversity is still poorly understood and underexplored (Rateb and Abdelmohsen, 2021).

The isolation and structure elucidation of thuwalamides A–E (**1**, **3**, **5**, **6** and **8**), previously undescribed polychlorinated amides, along with ten previously reported related compounds (**2**, **4**, **7** and **9**–**15**) from the organic extract of the marine sponge *L. herbacea* collected from coral reefs off Thuwal in the central Red Sea, Saudi Arabia, as well as the

* Corresponding author.
E-mail addresses: mtammam@pharm.uoa.gr (M.A. Tammam), ntsoureas@chem.uoa.gr (N. Tsoureas), dafnid@pharm.uoa.gr (D.-I. Diakaki), carlos.duarte@kaust.edu.sa (C.M. Duarte), roussis@pharm.uoa.gr (V. Roussis), eioannou@pharm.uoa.gr (E. Ioannou).

https://doi.org/10.1016/j.phytochem.2024.114315
Received 30 August 2024; Received in revised form 5 November 2024; Accepted 6 November 2024
Available online 6 November 2024

evaluation of the antibacterial activity of the isolated compounds, are described herein.

2. Results and discussion

A series of chromatographic separations of the CH_2Cl_2/MeOH extract of the sponge *L. herbacea* collected from the coral reef off Thuwal in Saudi Arabia allowed for the isolation of compounds **1**–**15** (Fig. 1).

Thuwalamide A (**1**), isolated in the form of colourless crystals, possessed the molecular formula $C_{14}H_{21}Cl_6NO_2$ as deduced from the HR-APCIMS data (Fig. S6). Indeed, the presence of six chlorine atoms in the molecule was evidenced by the pseudomolecular ion peak $[M+H]^+$ cluster at *m/z* 445.9781, 447.9747, 449.9715, 451.9684, 453.9650 and 455.9618 with relative intensities 52:100:81:35:8:1, agreeing with the theoretical isotopic envelope. In addition, the absorption bands at 1720 and 1647 cm^{-1} observed in the IR spectrum indicated the presence of two carbonyl groups (Fig. S7). The ^1H and ^{13}C NMR and HSQC spectra (Fig. S1, Fig. S2 and Fig. S3) confirmed the presence of four methyls on tertiary carbon atoms, two methylenes, four methines, two carbonyl groups and two deshielded non-protonated carbons resonating at δ_C 104.8 and 105.3 (Table 1). As readily observed from the cross-peaks in the COSY spectrum (Fig. S5), evident was the presence of three short spin systems, H-2/H_2-3/H-4/H_3-9, H-7/H_3-8 (H_3-10) and H_2-2′/H-3′/H_3-5′ (Fig. 2). The HMBC correlations of H_2-3 (δ_H 2.05 and 1.77), H-4 (δ_H 2.57), and H_3-9 (δ_H 1.49) with C-5 (δ_C 105.3), of H-2 (δ_H 4.94), H-7 (δ_H 2.81), H_3-8 (δ_H 1.13), H_3-10 (δ_H 1.16) with C-6 (δ_C 211.7), of H-2, H_2-2′ (δ_H 3.03 and 2.26) and NH-1 (δ_H 6.23) with C-1′ (δ_C 170.4), as well as of H_2-2′ and H_3-5′ (δ_H 1.34) with C-4′ (δ_C 104.8) concluded the planar structure of compound **1** (Fig. S4), which was identified as a previously undescribed hexachlorinated amide named thuwalamide A. Single crystal X-ray diffraction studies of **1** (Fig. 3 and Table S1) confirmed the proposed structure and allowed for the unambiguous determination of its absolute stereochemistry as 2*S*,4*S*,3′*S*.

Compounds **2** and **3**, both obtained as colourless crystals, possessed the same molecular formula ($C_{16}H_{23}Cl_6NO_4$), as indicated by analysis of their mass spectrometric data. Their ^1H and ^{13}C NMR spectroscopic data, which were rather similar, included signals for two singlet methyls, two doublet methyls and one oxygenated methyl, two methylenes, three methines, three carbonyl groups and two deshielded non-protonated carbons (δ_C 104.8 and 105.4 for **3** vs. δ_C 104.8 and 105.3, respectively, for **2**), as well as one more non-protonated carbon (Table 1, Fig. S9, Fig. S10, Fig. S11 and Fig. S12). The correlations observed in their respective HSQC, HMBC and COSY spectra (Fig. S13, Fig. S14 and Fig. S15) suggested the same planar structure for **2** and **3** and led to the identification of compound **2** as a previously reported hexachlorinated amide (Sauleau et al., 2005). The fact that in the case of **3** H-2, H-3a and H-4 were deshielded (δ_H 5.19, 2.49 and 2.63, respectively, for **3** vs. δ_H 5.09, 2.14 and 2.47, respectively, for **2**) and H-3b and H_3-9 were shielded (δ_H 1.50 and 1.33, respectively, for **3** vs. δ_H 1.68 and 1.42, respectively, for **2**) suggested a change in the relative configuration at either C-2 or C-4 or both. Since compound **2**, for which the relative configuration had not been proposed, was isolated in crystalline form, it was submitted to single-crystal X-ray diffraction analysis (Fig. 3 and Table S1) and its absolute stereochemistry was determined as 2*S*,4*S*,3′*S*.

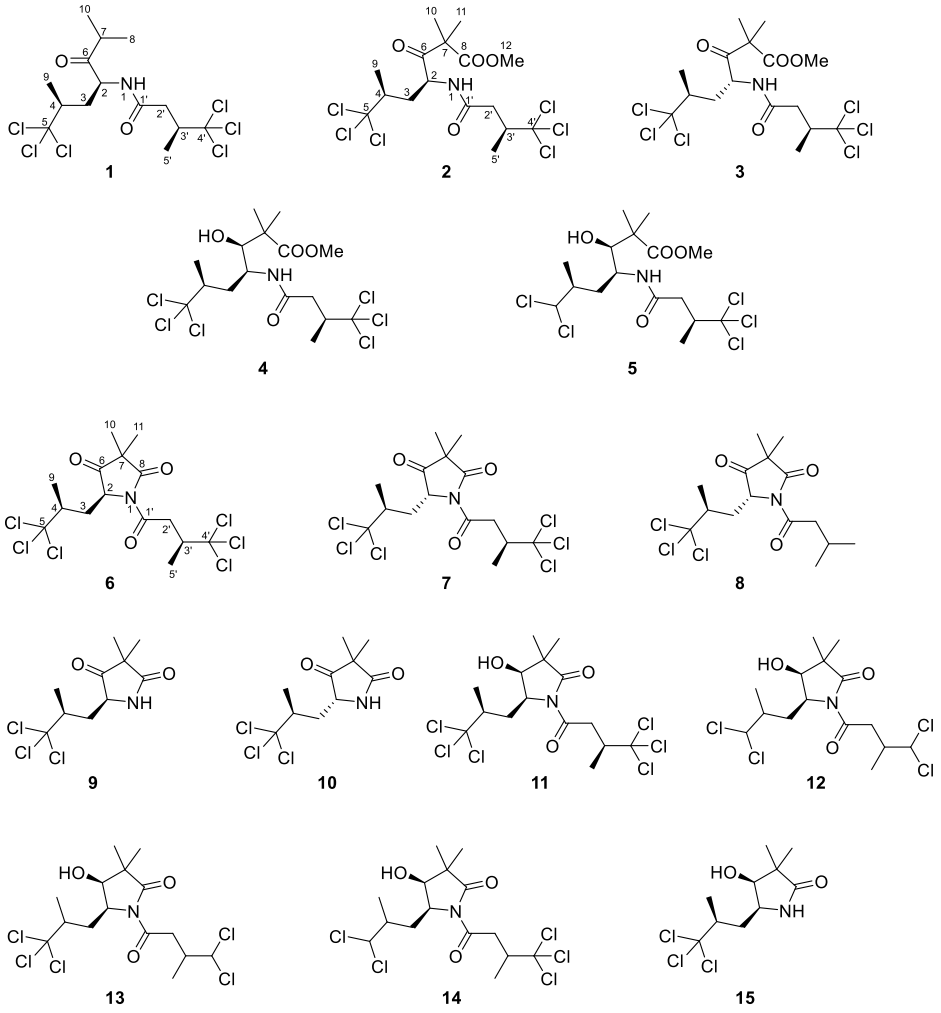

Fig. 1. Chemical structures of compounds **1–15**.

Table 1
^{1}H and ^{13}C NMR data (δ in ppm, J in Hz) of compounds **1**, **3**, **5**, **6** and **8** in $CDCl_3$.

Position	1		3		5		6		8	
	δ_C	δ_H	δ_C	δ_H	δ_C	δ_H	δ_C	δ_H	δ_C	δ_H
1	–	6.21 d (8.5)	–	5.93 d (8.5)	–	5.76 d (9.8)	–	–	–	–
2	53.8	4.94 ddd (12.6, 8.5, 2.4)	52.9	5.19 ddd (9.2, 8.5, 5.0)	46.3	4.30 m	62.6	4.60 t (5.5)	61.1	4.51 dd (8.8, 6.4)
3	36.3	2.05 t (12.6), 1.77 ddd (12.6, 10.2, 2.4)	36.5	2.49 ddd (14.6, 5.0, 2.6), 1.50 ddd (14.6, 9.2, 7.5)	38.0	2.11 m, 1.43 m	37.7	2.46 ddd (14.4, 5.5, 2.1), 1.92 ddd (14.4, 9.2, 5.5)	35.2	2.20 m
4	52.0	2.57 br dq (10.2, 6.4)	52.1	2.63 dqd (7.5, 6.7, 2.6)	40.8	2.05 m	52.7	3.02 ddd (9.2, 6.5, 2.1)	50.4	2.98 m
5	105.3	–	105.4	–	78.8	5.76 d (2.5)	105.0	–	105.1	–
6	211.7	–	207.0	–	79.0	3.58 d (6.1)	209.9	–	210.0	–
7	38.3	2.81 sep (7.0)	55.2	–	45.8	–	48.9	–	49.2	–
8	17.6	1.13 d (7.0)	173.0	–	179.2	–	176.3	–	175.9	–
9	16.4	1.49 d (6.4)	18.2	1.33 d (6.7)	15.6	1.20 d (6.7)	17.1	1.41 d (6.5)	15.8	1.47 d (6.5)
10	18.9	1.16 d (7.0)	22.0	1.43 s	20.1	1.19 s	20.9	1.32 s	20.8	1.29 s
11	–	–	22.1	1.44 s	24.1	1.28 s	22.0	1.36 s	22.7	1.38 s
12	–	–	52.86	3.73 s	52.2	3.70 s	–	–	–	–
1′	170.4	–	169.3	–	169.8	–	171.7	–	173.2	–
2′	40.2	3.03 dd (14.9, 2.7), 2.26 dd (14.9, 9.7)	40.1	2.98 dd (15.1, 2.4), 2.17 dd (15.1, 9.5)	40.5	2.90 dd (14.5, 2.5), 2.13 m	42.6	3.71 dd (18.3, 2.0), 3.20 dd (18.3, 9.3)	46.9	2.91 dd (16.5, 6.5), 2.83 dd (16.5, 7.1)
3′	51.7	3.18 dqd (9.7, 6.5, 2.7)	51.6	3.18 dqd (9.5, 6.5, 2.4)	51.4	3.16 dqd (12.0, 6.4, 2.5)	50.6	3.35 dqd (9.3, 6.5, 2.0)	24.9	2.18 m
4′	104.8	–	104.8	–	104.7	–	104.7	–	22.7	1.00 d (6.5)
5′	16.8	1.34 d (6.5)	16.8	1.30 d (6.5)	16.7	1.31 d (6.3)	17.3	1.39 d (6.5)	22.6	0.98 d (6.5)
OH	–	–	–	–	–	3.84 d (6.1)	–	–	–	–

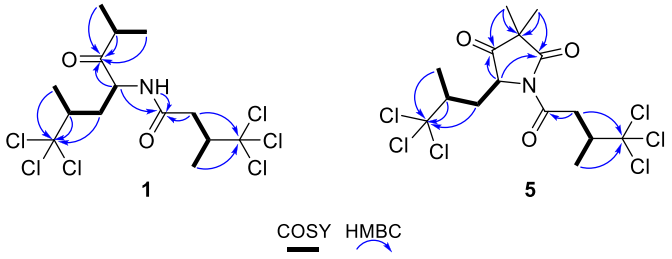

Fig. 2. COSY and important HMBC correlations observed for compounds **1** and **5**.

Moreover, single-crystal X-ray diffraction analysis of **3** (Fig. 3 and Table S1) established its absolute stereochemistry as 2*R*,4*S*,3′*S*, verifying that the previously undescribed compound **3**, named thuwalamide B, is the epimer of **2** at C-2. Careful interpretation of the spectroscopic data of compound **2** led to the conclusion that the chemical shift of C-7 should be 55.1 and not 40.5 ppm as previously assigned (Sauleau et al., 2005).

Thuwalamide C (**5**), obtained as colorless crystals, possessed the molecular formula $C_{16}H_{26}Cl_5NO_4$ as suggested by its HR-APCIMS data (Fig. S24), where the pseudomolecular ion peak $[M+H]^+$ cluster observed at *m/z* 472.0384, 474.0351, 476.0320, 478.0287 and 480.0251 with relative intensities 61:100:65:20:3 was indicative of the presence of five chlorine atoms in the molecule. The spectroscopic features of metabolite **5** shared a high degree of similarity with those of the co-occurring hexachlorinated amide **4**, previously reported from *L. herbacea* (Sauleau et al., 2005). The main difference was the replacement of one of the two deshielded non-protonated carbons in **4** by a deshielded methine at δ_H 5.76/δ_C 78.8 in metabolite **5**, suggesting the replacement of one CCl_3 terminal group in **4** by a $C(H)Cl_2$ moiety in **5** (Table 1, Fig. S19 and Fig. S20). This hypothesis was further confirmed by the COSY cross-peaks that dictated the presence of the spin system H-6/H-2/H_2-3/H-4 (H_3-9)/H-5, as well as the HMBC correlations of H-5 (δ_H 5.76) with C-3 (δ_C 38.0) and of H-3a (δ_H 1.43), H-4 (δ_H 2.05) and H_3-9 (δ_H 1.20) with C-5 (δ_C 78.8) (Fig. 2, Fig. S22 and Fig. S23). As in the case of compound **2**, the relative configuration of metabolite **4** had not been previously assigned. Therefore, successful crystallization of **4** enabled its single-crystal X-ray diffraction analysis (Fig. 3 and Table S1) and the determination of its absolute stereochemistry as 2*S*,4*S*,6*S*,3′*S*. Furthermore, the same absolute stereochemistry was established for the previously undescribed thuwalamide C (**5**) based on single-crystal X-ray diffraction analysis (Fig. 3 and Table S1).

Compounds **6** and **7** possessed the same molecular formula ($C_{15}H_{19}Cl_6NO_3$), based on analysis of their mass spectrometric data, indicating a monocyclic structure based on the four degrees of unsaturation and the presence of three carbonyl moieties. Their ^{1}H and ^{13}C NMR spectroscopic data, which shared a high degree of similarity, included signals for two singlet and two doublet methyls, two methylenes, three methines, three carbonyls and three non-protonated carbons, among which two were rather deshielded (δ_C 104.7 and 105.0 for **6** vs. δ_C 104.7 and 105.1, respectively, for **7**) (Table 1, Fig. S27, Fig. S28 and Fig. S35). The correlations observed in their respective HSQC, HMBC and COSY spectra (Fig. S29, Fig. S30 and Fig. S31) revealed the same planar structure for **6** and **7** and led to the identification of compound **7** as the previously reported hexachlorinated pyrrolidinone dysidamide H (Sauleau et al., 2005). As in the case of compounds **2** and **3**, protons H-2 and H-3a in **6** were deshielded compared to the ones in **7** (δ_H 4.60 and 2.46, respectively, for **6** vs. δ_H 4.52 and 2.20, respectively, for **7**), while H-3b and H_3-9 were shielded in **6** in comparison to those in **7** (δ_H 1.92 and 1.41, respectively, for **6** vs. δ_H 2.20 and 1.47, respectively, for **7**). This suggests a change in the configuration of the stereogenic centers. Indeed, single-crystal X-ray diffraction analysis of the previously undescribed thuwalamide D (**6**) (Fig. 3 and Table S1) established its absolute stereochemistry as 2*S*,4*S*,3′*S*. Unfortunately, a suitable crystal of dysidamide H (**7**), for which the relative configuration had not been proposed, could not be obtained for single-crystal X-ray diffraction experiments. Nevertheless, on the basis of biosynthetic considerations and taking into account that the stereochemistry at C-4 and C-3′ seems conserved throughout the series of these co-occurring metabolites as *S*,*S*, whereas the stereochemistry at C-2 can result in both epimers at this position, it is proposed that dysidamide H (**7**) possesses a 2*R*,4*S*,3′*S* absolute stereochemistry.

Thuwalamide E (**8**), isolated as a colorless oil, has the molecular formula $C_{15}H_{22}Cl_3NO_3$ as deduced from its HR-APCIMS and NMR data (Fig. S41). The ^{1}H and ^{13}C NMR data of compound **8** (Table 1, Fig. S36 and Fig. S37) included signals for two singlet and three doublet methyls, two methylenes, three methines, three carbonyls and two non-

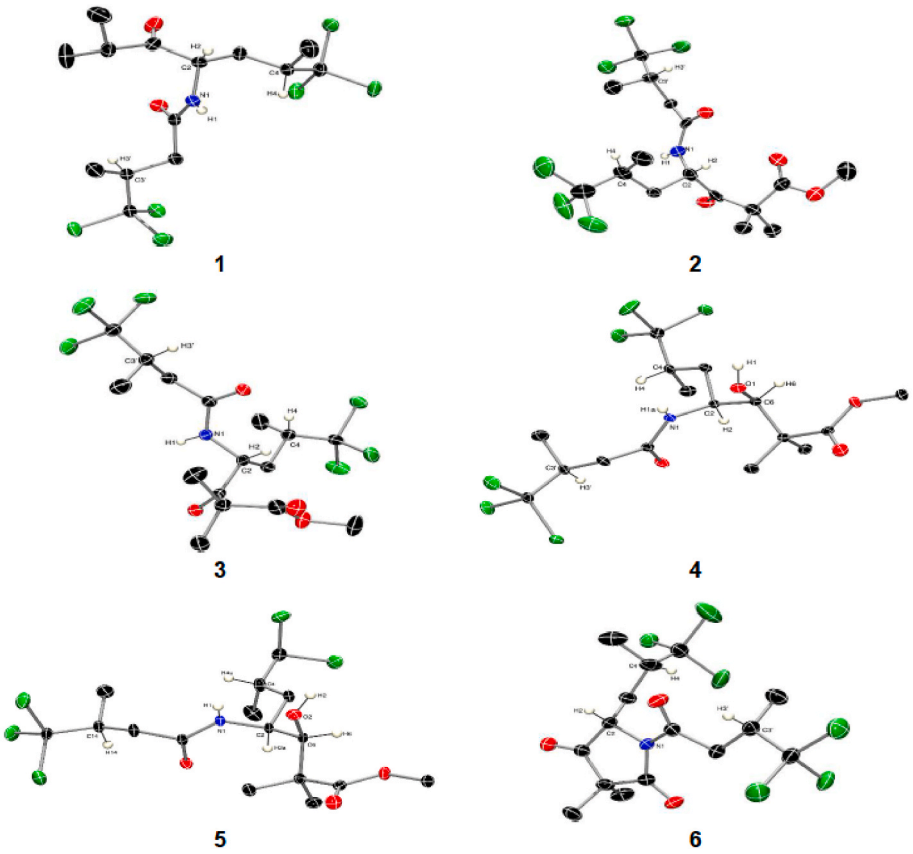

Fig. 3. ORTEP drawings showing 50% atomic displacement parameters (ADPs) of the molecular structures of compounds **1**–**6**.

protonated carbons, among which one was rather deshielded at δ_C 105.1. The COSY cross-peaks and HMBC correlations observed revealed a pyrrolidinone planar structure with the same side chain terminating with a CCl_3 moiety, as in **6** and **7**, attached to C-2, whereas the amide chain did not contain any chlorine atoms (Fig. S39 and Fig. S40). Attempts to crystallize compound **8** proved unsuccessful. However, the almost identical ^{1}H and ^{13}C NMR chemical shifts for H-2, H_2-3, H-4 and H_3-9, as well as C-2, C-3, C-4, C-5 and C-9, observed for the co-occurring compounds **7** and **8**, suggest that thuwalamide E (**8**) possesses a 2*R*, 4*S* stereochemistry.

The previously described compounds were identified by comparison of their spectroscopic and physical characteristics with those reported in the literature as 7,7,7-trichloro-2,2,6-trimethyl-3-oxo-4-(4,4,4-trichloro-3-methyl-1-oxobutylamino)-heptanoic acid methyl ester (**2**), 7,7,7-trichloro-3-hydroxy-2,2,6-trimethyl-4-(4,4,4-trichloro-3-methyl-1-oxobutylamino)-heptanoic acid methyl ester (**4**), dysidamide H (**7**), dysidamide G (**9**) and its epimer **10**, dysidamide (**11**), dysidamide B (**12**), and dysidamides D (**13**), E (**14**) and F (**15**) (Carmely et al., 1990; Gebreyesus et al., 1988; Isaacs et al., 1991; Sauleau et al., 2005).

Compounds **1**–**15** were evaluated for their antibacterial activity against the Gram-negative *Escherichia coli* strain NCTC-10418 and the Gram-positive *Staphylococcus aureus* strain ATCC-25923 (Table S2). The tested compounds could not inhibit the growth of *E. coli* up to a concentration of 128 μg/mL. On the other hand, compounds **12** and **13** displayed weak to moderate inhibitory activity against *S. aureus* with MIC values of 64 and 32 μg/mL, respectively, while dysidamide E (**14**) was proven more effective with a MIC value of 4 μg/mL, similarly to vancomycin that was used as a positive control.

3. Conclusions

The chemical investigation of the organic extract of the sponge *L. herbacea*, collected off the village of Thuwal in the Red Sea at Saudi Arabia, led to the isolation and structure elucidation of 15 polychlorinated amides. Among them, thuwalamides A–E (**1**, **3**, **5**, **6** and **8**) represent previously undescribed natural products, whereas compounds **2**, **4**, **7** and **9**–**15** have been previously reported in the relevant literature. The structures of thuwalamides A–E were determined on the basis of thorough analysis of their NMR and MS data, while their absolute stereochemistry was established on the basis of single crystal X-ray diffraction analysis. Additionally, the relative configuration and the absolute stereochemistry of the previously reported compounds **2** and **4**, which had not been assigned, were determined based on analysis of their X-ray crystallographic data. Among compounds **1**–**15**, dysidamide E (**14**) displayed activity against *S. aureus* comparable to vancomycin that was used as a positive control with a MIC value of 4 μg/mL.

4. Experimental

4.1. General experimental procedures

Optical rotations were measured on a Krüss model P3000 polarimeter (A. KRÜSS Optronic GmbH, Hamburg, Germany) with a 0.5 dm cell. UV spectra were recorded on Shimadzu UV-1900i UV–Vis spectrophotometer (Shimadzu Europa GmbH, Duisburg, Germany). IR spectra were obtained on an Alpha II FTIR spectrometer (Bruker Optik GmbH, Ettlingen, Germany). High-resolution APCI mass spectra were measured on a LTQ Orbitrap Velos mass spectrometer (Thermo Fisher Scientific, Bremen, Germany). NMR spectra were recorded on a Bruker DRX 400 (Bruker BioSpin GmbH, Rheinstetten, Germany) spectrometer. Chemical shifts are given on the δ (ppm) scale with reference to the solvent signals. The 2D NMR experiments (HSQC, HMBC, COSY, NOESY) were performed using standard Bruker pulse sequences. Column chromatography separations were performed with Kieselgel 60 (Merck, Darmstadt,

Germany). HPLC separations were conducted on a LKB 2248 liquid chromatography pump (Pharmacia LKB Biotechnology, Uppsala, Sweden) equipped with a Shodex RI-102 refractive index detector (ECOM spol. s r.o., Prague, Czech Republic) using a Supelcosil SPLC-Si 5 μm (250 × 10 mm) column (Supelco, Bellefonte, PA, USA) or on a Waters 600 liquid chromatography pump (Waters, Milford, MA, USA) with a Waters 410 refractive index detector (Waters, Milford, MA, USA) using a Kromasil 100 C_{18} (250 mm × 8 mm) column (MZ-Analysentechnik GmbH, Mainz, Germany). TLC was performed with Kieselgel 60 F_{254} (Merck aluminum-backed plates) and spots were detected after spraying with 15% H_2SO_4 in MeOH reagent and heating at 100 °C for 1 min.

4.2. Animal material

Specimens of the sponge *L. herbacea* (Keller) were hand-picked off the village of Thuwal, Saudi Arabia, at a depth of 1–2 m, in January of 2018. A voucher specimen has been deposited at the animal collection of the Section of Pharmacognosy and Chemistry of Natural Products, Department of Pharmacy, National and Kapodistrian University of Athens (ATPH/MP0649).

4.3. Extraction and isolation

The fresh specimens of the sponge were extensively extracted with mixtures of CH_2Cl_2 and MeOH at room temperature, to afford after evaporation of the solvents in vacuo a crude extract (15.8 g) that was subjected to vacuum column chromatography on silica gel, using cHex with increasing amounts of EtOAc, followed by EtOAc with increasing amounts of MeOH as the mobile phase, to yield seven fractions (A-G). Fractions B and C (20–60% EtOAc in cHex, 2.33 and 2.62 g, respectively) were combined and further separated by gravity column chromatography on silica gel, using mixtures of cHex and EtOAc of increasing polarity as the mobile phase to afford 16 fractions (B1–B16). Fraction B5 (10% EtOAc in cHex, 72.5 mg) was subjected to normal-phase vacuum column chromatography, using cHex with increasing amounts of Me_2CO as the eluent, to yield two fractions (B5a-B5b). Fraction B5a (5–7% Me_2CO in cHex, 67.5 mg) was further fractionated by normal-phase vacuum column chromatography, using cHex with increasing amounts of EtOAc as the mobile phase, to afford two fractions (B5a1-B5a2). Fraction B5a1 (5–10% EtOAc in cHex, 57.5 mg) was repeatedly subjected to normal-phase HPLC with cHex/EtOAc (96:4) and cHex/Me_2CO (98:2 and 96:4) as the eluent to yield compounds **6** (1.3 mg, t_R = 20.5 min in cHex/Me_2CO, 98:2, 1.5 mL/min), **7** (10.0 mg, t_R = 18.7 min in cHex/EtOAc, 96:4, 1.5 mL/min) and **8** (0.7 mg, t_R = 14.3 min in cHex/Me_2CO, 96:4, 1.5 mL/min). Fraction B6 (10–12% EtOAc in cHex, 63.5 mg) was further fractionated by normal-phase vacuum column chromatography, using cHex with increasing amounts of EtOAc as the mobile phase, to afford three fractions (B6a-B6c). Fraction B6a (4–8% EtOAc in cHex, 18.7 mg) was subjected to normal-phase HPLC using cHex/EtOAc (93:7) and subsequently cHex/Me_2CO (98:2) as the mobile phase to yield compounds **6** (2.4 mg, t_R = 14.3 min in cHex/EtOAc, 93:7, 1.5 mL/min), **7** (6.9 mg, t_R = 16.6 min in cHex/EtOAc, 93:7, 1.5 mL/min) and **8** (1.2 mg, t_R = 20.5 min in cHex/Me_2CO, 98:2, 1.5 mL/min). Fraction B6b (10% EtOAc in cHex, 36.3 mg) was subjected to normal-phase HPLC using cHex/EtOAc (93:7) and subsequently cHex/Me_2CO (96:4) as the eluent to yield compounds **1** (1.9 mg, t_R = 19.1 min in cHex/Me_2CO, 96:4, 1.5 mL/min) and **7** (4.2 mg, t_R = 16.6 min in cHex/EtOAc, 93:7, 1.5 mL/min). Fraction B7 (12% EtOAc in cHex, 39.5 mg) was subjected to vacuum column chromatography on silica gel, using cHex with increasing amounts of EtOAc as the mobile phase, to afford three fractions (B7a-B7c). Fraction B7b (7–8% EtOAc in c-Hex, 11.0 mg) was further fractionated with normal-phase HPLC using cHex/EtOAc (93:7) and subsequently cHex/Me_2CO (96:4) as the eluent to yield compound **2** (1.0 mg, t_R = 23.6 min in cHex/Me_2CO, 96:4, 1.5 mL/min). Fraction B8 (12–16% EtOAc in cHex, 181.7 mg), was subjected to normal-phase vacuum column chromatography, using cHex with increasing amounts of EtOAc as the mobile phase, to afford six fractions (B8a-B8f). Fraction B8b (7–8% EtOAc in cHex, 95.2 mg) was submitted to normal-phase HPLC using cHex/EtOAc (93:7), cHex/Me_2CO (96:4 and 94:6) and subsequently *n*-Hex/Me_2CO (96:4) as eluent to yield compound **2** (9.0 mg, t_R = 23.6 min in cHex/Me_2CO, 96:4, 1.5 mL/min) and **3** (9.2 mg, t_R = 23.8 min in *n*-Hex/Me_2CO, 96:4, 1.5 mL/min). Fraction B8e (8% EtOAc in cHex, 8.4 mg) was fractionated by normal-phase HPLC using cHex/Me_2CO (94:6) as eluent to yield compound **11** (2.0 mg, t_R = 21.2 min in cHex/Me_2CO, 94:6, 1.5 mL/min). Fraction B9 (16–20% EtOAc in cHex, 3.4 g) was fractionated by gravity column chromatography on silica gel using mixtures of toluene and Me_2CO of increasing polarity as the mobile phase to yield fourteen fractions (B9a-B9n). Fraction B9f (4% Me_2CO in toluene, 1.8 g) was repeatedly submitted to normal-phase HPLC using toluene/Me_2CO (96:4) as eluent to yield compounds **4** (3.9 mg, t_R = 20.0 min in toluene/Me_2CO, 96:4, 1.5 mL/min) and **11** (1.2 g, t_R = 17.5 min in toluene/Me_2CO, 96:4, 1.5 mL/min). Fraction B9g (4% Me_2CO in toluene, 634.6 mg) was repeatedly subjected to normal-phase HPLC using toluene/Me_2CO (96:4) and cHex/Me_2CO (90:10) as eluent to afford **4** (24.4 mg, t_R = 20.0 min in toluene/Me_2CO, 96:4, 1.5 mL/min), **11** (352.3 mg, t_R = 17.5 min in toluene/Me_2CO, 96:4, 1.5 mL/min) and **14** (6.0 mg, t_R = 22.9 min in cHex/Me_2CO, 90:10, 1.5 mL/min). Fraction B9h (4–5% Me_2CO in toluene, 357.0 mg) was repeatedly subjected to normal-phase HPLC using toluene/Me_2CO (96:4), cHex/Me_2CO (90:10) and *n*-Hex/Me_2CO (88:12) as the eluent to yield **4** (41.1 mg, t_R = 23.4 min in cHex/Me_2CO, 90:10, 1.2 mL/min), **5** (0.5 mg, t_R = 24.9 min in *n*-Hex/Me_2CO, 88:12, 1.5 mL/min), **11** (86.4 mg, t_R = 22.5 min in cHex/Me_2CO, 90:10, 1.2 mL/min), **12** (1.4 mg, t_R = 19.5 min in toluene/Me_2CO, 96:4, 1.5 mL/min), **13** (10.8 mg, t_R = 25.1 min in cHex/Me_2CO, 90:10, 1.2 mL/min) and **14** (13.4 mg, t_R = 24.1 min in cHex/Me_2CO, 90:10, 1.2 mL/min). Fraction B9i (5% Me_2CO in toluene, 54.2 mg) was fractionated with normal-phase HPLC using toluene/Me_2CO (95:5) as the mobile phase to yield compounds **11** (2.5 mg, t_R = 14.7 min in toluene/Me_2CO, 95:5, 1.5 mL/min) and **13** (7.2 mg, t_R = 15.8 min in toluene/Me_2CO, 95:5, 1.5 mL/min). Fraction B9j (5–6% Me_2CO in toluene, 37.8 mg) was purified by normal-phase HPLC eluting with toluene/Me_2CO (95:5) to afford compound **13** (1.6 mg, t_R = 15.8 min in toluene/Me_2CO, 95:5, 1.5 mL/min). Fractions E, F and G (90–100% EtOAc in cHex and 10–100% MeOH in EtOAc, 1.44g) were combined and further separated by gravity column chromatography on silica gel, using cHex with increasing amounts of EtOAc followed by EtOAc with increasing amounts of MeOH, to yield ten fractions (E1-E10). Fraction E4 (45% EtOAc in cHex, 40.1 mg) was submitted to normal-phase HPLC using cHex/EtOAc (45:55) as the eluent to afford compound **9** (2.0 mg, t_R = 18.3 min in cHex/EtOAc, 45:55, 1.5 mL/min) and a fraction that was subsequently subjected to reversed-phase HPLC eluting with MeOH (100%) to afford compound **10** (2.5 mg, t_R = 8.8 min MeOH, 100%, 1.5 mL/min). Fraction E5 (45–50% EtOAc in cHex, 152.6 mg) was fractionated with normal-phase HPLC using cHex/EtOAc (45:55) as the eluent to yield a fraction that was subsequently purified by reversed-phase HPLC using MeOH (100%) as eluent to yield **10** (2.3 mg, t_R = 8.8 min MeOH, 100%, 1.5 mL/min). Fraction E7 (70–80% EtOAc in cHex, 123.4 mg) was fractionated with normal-phase HPLC eluting with cHex/EtOAc (45:55) to afford a fraction that was subsequently subjected to reversed-phase HPLC using MeOH/H_2O (95:5 and 92:8) as eluent to yield compound **15** (14.5 mg, t_R = 13.2 min MeOH/H_2O, 92:8, 1.5 mL/min).

4.3.1. Thuwalamide A (1)

Colourless crystals; $[\alpha]_D^{20}$ +3.33 (*c* 0.12, $CHCl_3$); UV (MeOH) λ_{max} (log ε) 207.0 (3.51) nm; IR (thin film) ν_{max} 2974, 2933, 1720, 1647, 1536, 1463, 1348, 797, 765; ^1H and ^{13}C NMR data, see Table 1; HR-APCIMS *m/z* 445.9781 $[M+H]^+$ (calcd. for $C_{14}H_{22}^{35}Cl_6NO_2$, 445.9782).

4.3.2. Thuwalamide B (3)

Colourless crystals; $[\alpha]_D^{20}$ +6.05 (*c* 0.33, $CHCl_3$); UV (MeOH) λ_{max}

(log ε) 207.0 (3.55) nm; IR (thin film) ν_{max} 3298, 2948, 1752, 1717, 1650, 1536, 1279, 1153, 791, 768; ^{1}H and ^{13}C NMR data, see Table 1; HR-APCIMS *m/z* 503.9839 $[M+H]^+$ (calcd. for $C_{16}H_{24}^{35}Cl_6NO_4$, 503.9836).

4.3.3. Thuwalamide C (5)

Colourless crystals; $[\alpha]_D^{20}$ -75.0 (*c* 0.027, $CHCl_3$); UV (MeOH) λ_{max} (log ε) 202.0 (3.50) nm; IR (thin film) ν_{max} 3351, 2927, 1726, 1525, 1463, 1709, 1262, 1142, 1095, 800,771, 753, 698; ^{1}H and ^{13}C NMR data, see Table 1; HR-APCIMS *m/z* 472.0384 $[M+H]^+$ (calcd. for $C_{16}H_{27}^{35}Cl_5NO_4$, 472.0383).

4.3.4. Thuwalamide D (6)

Colourless crystals; $[\alpha]_D^{20}$ +13.04 (*c* 0.15, $CHCl_3$); UV (MeOH) λ_{max} (log ε) 219.0 (3.59) nm; IR (thin film) ν_{max} 2936, 1779, 1741, 1709, 1381, 1367, 1168, 771; ^{1}H and ^{13}C NMR data, see Table 1; HR-APCIMS *m/z* 471.9571 $[M+H]^+$ (calcd. for $C_{15}H_{20}^{35}Cl_6NO_3$, 471.9574).

4.3.5. Thuwalamide E (8)

Colourless oil; $[\alpha]_D^{20}$ -54.55 (*c* 0.073, $CHCl_3$); UV (MeOH) λ_{max} (log ε) 219.0 (3.44) nm; IR (thin film) ν_{max} 2959, 2927, 1775, 1734, 1708, 1465, 1164, 1033, 793, 770; ^{1}H and ^{13}C NMR data, see Table 1; HR-APCIMS *m/z* 370.0742 $[M+H]^+$ (calcd. for $C_{15}H_{23}^{35}Cl_3NO_3$, 370.0744).

4.4. Single-crystal X-ray diffraction analysis

Compounds **1**–**6** were crystallized by slow evaporation of saturated solutions of MeOH, either as colourless plates (**1**, **4** and **6**), colourless rods (**2** and **3**) or colourless flakes (**5**). Data for compounds **1**–**6** were collected on a dual source (IμS Diamond Cu/Kα & Mo/Kα) Bruker D8-Venture SC-XRD instrument equipped with a Photon-III area detector at 100K using an Oxford Cryosystems 100 cryostream. Data were collected using φ and ω scans to fill the Ewald sphere using a 4-circle kappa goniometer. Data collection and subsequent processing were handled by the APEX4 software package. A multi-scan absorption correction (SADABS, 2016/2) was applied in all cases unless otherwise stated. Data solution (ShelXT: Sheldrick, 2015a or Superflip: Palatinus and Chapuis, 2007) and model refinement (ShelXL: Sheldrick, 2008; Sheldrick, 2015b) were achieved using the Olex2-1.5 software package (Dolomanov et al., 2009). All atoms were refined anisotropically and hydrogen atoms were added using the riding model, unless otherwise stated.

In the case of compound **1**, data were collected using Mo/Kα to a resolution of 0.75 Å. Two chlorine atoms in one of the CCl_3 moieties show occupational disorder (*ca* 63:27) which was modelled using the PART command and SADI restraints. The hydrogen connected to the nitrogen atom was located in the Fourier difference map and its position refined freely.

In the case of compound **2**, data were collected using Cu/Kα only to a resolution of 1.05 Å (THETM01_ALERT_3_A and PLAT340_ALERT_3_B) partly, due to the small size of the crystal, but mostly due to extensive radiation damage even at 100 K which rendered most of the sweeps of the data-collection devoid of any meaningful data. Despite this, the quality of the data is sufficient to establish the connectivity map, while the completeness to this resolution and the multiplicity (4.4) of the data were sufficient enough (PLAT089_ALERT_3_B) to establish the chirality of the molecule. Finally, the model was refined as a two component (87:13) merohedral twin (twin matrix: 1 -1 0 0 1 0 0 0–1 as established by PLATON TWINROTMAT (Spek, 2009).

In the case of compound **3**, data were collected using Mo/Kα to a resolution of 0.75 Å. A numerical absorption (Clark and Reid, 1995) based on crystal faces was applied after integration. There are two molecules in the asymmetric unit, with one of them showing occupational disorder between the ester moiety and one of the methyls attached to the quaternary carbon C31. This was modelled using the PART command and the occupancy of the two sites refined freely and found to be *ca* 64:36. Carbon atoms C19, C15 were isotropically refined and their counterparts in PART2 (ie C19A and C15A) were constrained to their ADP's respectively using the EADP command. The hydrogen connected to N2 was found in the Fourier difference map and was refined freely. In the case of N1, electron corresponding to its hydrogen was also located in the Fourier difference map, but in this case free refinement of its position led to a non-converging refinement. Therefore, this hydrogen (H1) was added using the riding model. These two N–H distances are similar within esd's (d(N1–H1) = 0.88 Å; d(N2–H2) = 0.88(7) Å).

In the case of compound **4**, data were collected using Mo/Kα to a resolution of 0.75 Å. The hydrogen connected to the nitrogen atom was located in the Fourier difference map and its position refined freely.

In the case of compound **5**, data were collected using Mo/Kα to a resolution of 0.75 Å. A numerical absorption based on crystal faces was applied after integration. The CH_2Cl_2 moiety was modelled as having occupational disorder over two sites (*ca* 95:5) using the PART command with the use of ISOR and SADI restraints, as well as constraining the ADP of Cl1a and C5a in PART 2 to their counterparts Cl1 and C5 in PART 1. The hydrogen connected to the nitrogen atom was located in the Fourier difference map and its position refined freely.

In the case of compound **6**, data were collected using Cu/Kα only to a resolution of 0.83 Å. As in the case of **2**, the crystals were prone to irradiation damage even at 100K. This led to more than half of the frames containing very little data, as well as the data completion being rather low for this resolution (97.4% for the Laue group and 90.6% for the point group - PLAT029_ALERT_3_C & PLAT911_ALERT_3_C). Nevertheless, the connectivity map and the chirality of the molecule could be established and agrees with the spectroscopic data for this compound.

Collection, data and final model refinement parameters are summarised in tabular form in Table S1.

4.4.1. Crystallographic data of thuwalamide A (1)

Colourless plates of **1** were crystallized by slow evaporation of a saturated methanolic solution, $C_{14}H_{21}Cl_6NO_2$ (M = 448.02 g/mol): monoclinic, space group $P2_1$, a = 9.1221(9) Å, b = 9.6825(8) Å, c = 12.1270(12) Å, $\alpha = 90°$, $\beta = 108.946(4)°$, $\gamma = 90°$, $V = 1013.09(17)$ Å^3, $Z = 2$, $T = 100$ K, μ(Mo Kα) = 0.854 mm^{-1}, ρ_{calc} = 1.469 g cm^{-3}, 74371 reflections measured ($2.361° \leq 2\theta \leq 28.282°$), 4735 independent reflections (R_{int} = 0.0851, R_{sigma} = 0.0332) which were used in all calculations. The final R_1 was 0.0574 ($I > 2\sigma(I)$) and wR_2 was 0.1535 ($I > 2\sigma(I)$). The Flack and Hooft parameters were 0.04(11) and 0.03(3), respectively. The X-ray structure (CIF) data of **1** (CCDC 2375956) has been deposited in the Cambridge Crystallographic Data Centre.

4.4.2. Crystallographic data of 7,7,7-trichloro-2,2,6-trimethyl-3-oxo-4-(4,4,4-trichloro-3-methyl-1-oxobutylamino)-heptanoic acid methyl ester (2)

Colourless rods of **2** were crystallized by slow evaporation of a saturated methanolic solution, $C_{16}H_{23}Cl_6NO_4$ (M = 506.05 g/mol): hexagonal, space group $P6_5$, a = 12.0760(6) Å, b = 12.0760(6) Å, c = 27.407(3) Å, $\alpha = 90°$, $\beta = 90°$, $\gamma = 120°$, $V = 3461.3(5)$ Å^3, $Z = 6$, T = 100 K, μ(Cu Kα) = 6.983 mm^{-1}, ρ_{calc} = 1.457 g cm^{-3}, 9247 reflections measured ($3.225° \leq 2\theta \leq 47.309°$), 1763 independent reflections (R_{int} = 0.0928, R_{sigma} = 0.0745) which were used in all calculations. The final R_1 was 0.0520 ($I > 2\sigma(I)$) and wR_2 was 13.30 ($I > 2\sigma(I)$). The Flack and Hooft parameters were 0.01(6) and 0.027(17), respectively. The X-ray structure (CIF) data of **2** (CCDC 2375958) has been deposited in the Cambridge Crystallographic Data Centre.

4.4.3. Crystallographic data of thuwalamide B (3)

Colourless rods of **3** were crystallized by slow evaporation of a saturated methanolic solution, $C_{16}H_{23}Cl_6NO_4$ (M = 506.05 g/mol): tetragonal, space group $P4_3$, a = 16.1531(8) Å, b = 16.1531(8) Å, c = 17.7148(11) Å, $\alpha = 90°$, $\beta = 90°$, $\gamma = 90°$, $V = 4622.2(5)$ Å^3, $Z = 8$, T = 100 K, μ(Mo Kα) = 0.764 mm^{-1}, ρ_{calc} = 1.454 g cm^{-3}, 116782 reflections measured ($2.122° \leq 2\theta \leq 28.292°$), 9547 independent

reflections (R_{int} = 0.0867, R_{sigma} = 0.0431) which were used in all calculations. The final R_1 was 0.037 (I > 2σ(I)) and wR_2 was 0.0880 (I > 2σ(I)). The Flack and Hooft parameters were −0.01(5) and −0.04(2), respectively. The X-ray structure (CIF) data of **3** (CCDC 2375959) has been deposited in the Cambridge Crystallographic Data Centre.

4.4.4. Crystallographic data of 7,7,7-trichloro-3-hydroxy-2,2,6-trimethyl-4-(4,4,4-trichloro-3-methyl-1-oxobutylamino)-heptanoic acid methyl ester (4)

Colourless plates of **4** were crystallized by slow evaporation of a saturated methanolic solution, $C_{16}H_{25}Cl_6NO_4$ (M = 508.07 g/mol): monoclinic, space group $P2_1$, a = 6.6450(8) Å, b = 9.2883(11) Å, c = 18.112(2) Å, $\alpha = 90°$, $\beta = 90.675(5)°$, $\gamma = 90°$, $V = 1117.8(2)$ Å^3, $Z = 2$, T = 100 K, μ(Mo Kα) = 0.790 mm^{-1}, ρ_{calc} = 1.510 g cm^{-3}, 33457 reflections measured ($2.464° \leq 2\theta \leq 28.412°$), 5073 independent reflections (R_{int} = 0.0585, R_{sigma} = 0.0397) which were used in all calculations. The final R_1 was 0.0397 (I > 2σ(I)) and wR_2 was 0.0900 (I > 2σ(I)). The Flack and Hooft parameters were −0.00(2) and 0.002(3), respectively. The X-ray structure (CIF) data of **4** (CCDC 2375957) has been deposited in the Cambridge Crystallographic Data Centre.

4.4.5. Crystallographic data of thuwalamide C (5)

Colourless flakes of **5** were crystallized by slow evaporation of a saturated methanolic solution, $C_{16}H_{26}Cl_5NO_4$ (M = 473.63 g/mol): monoclinic, space group $P2_1$, a = 6.7245(8) Å, b = 9.1244(12) Å, c = 17.628(2) Å, $\alpha = 90°$, $\beta = 94.210(5)°$, $\gamma = 90°$, $V = 1078.7(2)$ Å^3, $Z = 2$, T = 100 K, μ(Mo Kα) = 0.693 mm^{-1}, ρ_{calc} = 1.458 g cm^{-3}, 46158 reflections measured ($2.317° \leq 2\theta \leq 28.244°$), 4997 independent reflections (R_{int} = 0.0751, R_{sigma} = 0.0401) which were used in all calculations. The final R_1 was 0.0658 (I > 2σ(I)) and wR_2 was 0.1726 (I > 2σ(I)). The Flack and Hooft parameters were −0.06(12) and 0.04(2), respectively. The X-ray structure (CIF) data of **5** (CCDC 2375960) has been deposited in the Cambridge Crystallographic Data Centre.

4.4.6. Crystallographic data of thuwalamide D (6)

Colourless plates of **6** were crystallized by slow evaporation of a saturated methanolic solution, $C_{15}H_{19}Cl_6NO_3$ (M = 474.01 g/mol): monoclinic, space group $P2_1$, a = 9.8608(13) Å, b = 12.0788(17) Å, c = 9.9336(13) Å, $\alpha = 90°$, $\beta = 118.948(6)°$, $\gamma = 90°$, $V = 1035.3(2)$ Å^3, Z = 2, T = 100 K, μ(Cu Kα) = 7.705 mm^{-1}, ρ_{calc} = 1.521 g cm^{-3}, 7504 reflections measured ($5.088° \leq 2\theta \leq 67.679°$), 2961 independent reflections (R_{int} = 0.0575, R_{sigma} = 0.0638) which were used in all calculations. The final R_1 was 0.0525 (I > 2σ(I)) and wR_2 was 0.1302 (I > 2σ(I)). The Flack and Hooft parameters were 0.02(4) and 0.024(16), respectively. The X-ray structure (CIF) data of **6** (CCDC 2375955) has been deposited in the Cambridge Crystallographic Data Centre.

4.5. Evaluation of antibacterial activity

The antibacterial activity of the isolated compounds was evaluated against the bacterial strains *S. aureus* ATCC-25923 and *E. coli* NCTC-10418 using the methodology previously described (Dimou et al., 2016).

Funding

This research was partially supported by the Subaward Agreement Ref. OSR-2017-CPF-3627-2 funded by the King Abdullah University of Science and Technology.

CRediT authorship contribution statement

Mohamed A. Tammam: Writing – original draft, Visualization, Investigation. **Nikolaos Tsoureas:** Writing – original draft, Visualization, Methodology, Investigation. **Dafni-Ioanna Diakaki:** Investigation. **Carlos M. Duarte:** Writing – review & editing, Funding acquisition. **Vassilios Roussis:** Writing – review & editing, Supervision, Resources, Methodology, Funding acquisition. **Efstathia Ioannou:** Writing – review & editing, Writing – original draft, Supervision, Resources, Project administration, Methodology, Funding acquisition, Conceptualization.

Declaration of Competing Interest

The authors declare that they have no known competing financial interests or personal relationships that could have appeared to influence the work reported in this paper.

Acknowledgements

The authors would like to acknowledge the National and Kapodistrian University of Athens Core Facility for access to SC-XRD instrumentation. Access to the infrastructure obtained by the research project “Center for the study and sustainable exploitation of Marine Biological Resources” (CMBR, MIS 5002670) in the framework of the National Roadmap for Research Infrastructures is gratefully acknowledged.

Appendix B. Supplementary data

Supplementary data to this article can be found online at https://doi.org/10.1016/j.phytochem.2024.114315.

Data availability

Data will be made available on request.

References

Carmely, S., Gebreyesus, T., Kashman, Y., Skelton, B.W., White, A.H., Yosief, T., 1990. Dysidamide, a novel metabolite from a Red Sea sponge *Dysidea herbacea*. Aust. J. Chem. 43, 1881–1888. https://doi.org/10.1071/CH9901881.

Carroll, A.R., Copp, B.R., Grkovic, T., Keyzers, R.A., Prinsep, M.R., 2024. Marine natural products. Nat. Prod. Rep. 41, 162–207. https://doi.org/10.1039/D3NP00061C and previous reviews in this series.

Clark, R.C., Reid, J.S., 1995. The analytical calculation of absorption in multifaceted crystals. Acta Crystallogr. Sect. A. 51, 887–897. https://doi.org/10.1107/S0108767395007367.

de Voogd, N.J., Alvarez, B., Boury-Esnault, N., Cárdenas, P., Díaz, M.-C., Dohrmann, M., Downey, R., Goodwin, C., Hajdu, E., Hooper, J.N.A., Kelly, M., Klautau, M., Lim, S. C., Manconi, R., Morrow, C., Pinheiro, U., Pisera, A.B., Ríos, P., Rützler, K., Schönberg, C., Turner, T., Vacelet, J., van Soest, R.W.M., Xavier, J., 2024. World Porifera database. In: *Lamellodysidea* Cook & Bergquist, 2002. Accessed through: World Register of Marine Species at: https://www.marinespecies.org/aphia.php?p=taxdetails&id=164987on2024-08-01.

Dimou, M., Ioannou, E., Daskalaki, M.G., Tziveleka, L.A., Kampranis, S.C., Roussis, V., 2016. Disulfides with anti-inflammatory activity from the brown alga *Dictyopteris membranacea*. J. Nat. Prod. 79, 584–589. https://doi.org/10.1021/acs.jnatprod.5b01031.

Dolomanov, O.V., Bourhis, L.J., Gildea, R.J., Howard, J.A.K., Puschmann, H., 2009. OLEX2: a complete structure solution, refinement and analysis program. J. Appl. Crystallogr. 42, 339–341. https://doi.org/10.1107/S0021889808042726.

Fathallah, N., Tamer, A., Ibrahim, R., Kamal, M., Kes, M.E., 2023. The marine sponge genus *Dysidea* sp: the biological and chemical aspects-a review. Futur. J. Pharm. Sci. 9, 98. https://doi.org/10.1186/s43094-023-00550-9.

Gebreyesus, T., Yosief, T., Carmely, S., Kashman, Y., 1988. Dysidamide, a novel hexachloro-metabolite from a Red Sea sponge *Dysidea* sp. Tetrahedron Lett. 31, 3863–3864. https://doi.org/10.1016/S0040-4039(00)82135-8.

Hong, L.L., Ding, Y.F., Zhang, W., Lin, H.W., 2022. Chemical and biological diversity of new natural products from marine sponges: a review (2009-2018). Mar. Life Sci. Tech. 4, 356–372. https://doi.org/10.1007/s42995-022-00132-3.

Isaacs, S., Berman, R., Kashman, Y., Gebreyesus, T., Yosief, T., 1991. New polyhydroxy sterols, dysidamides, and a dideoxyhexose from the sponge *Dysidea herbacea*. J. Nat. Prod. 54, 83–91. https://doi.org/10.1021/np50073a004.

MarinLit. 2024. Available online: https://marinlit.rsc.org/(accessed on 15 July 2024).

Palatinus, L., Chapuis, G., 2007. SUPERFLIP-a computer program for the solution of crystal structures by charge flipping in arbitrary dimensions. J. Appl. Cryst. 40, 786–790. https://doi.org/10.1107/S0021889807029238.

Rateb, M.E., Abdelmohsen, U.R., 2021. Bioactive natural products from the Red Sea. Mar. Drugs 19, 289–292. https://doi.org/10.3390/md19060289.

Sauleau, P., Bourguet-Kondracki, M.-L.L., 2005. Novel polyhydroxysterols from the Red Sea marine sponge *Lamellodysidea herbacea*. Steroids 70, 954–959. https://doi.org/10.1016/j.steroids.2005.07.004.

Sauleau, P., Retailleau, P., Vacelet, J., Bourguet-Kondracki, M.-L.L., 2005. New polychlorinated pyrrolidinones from the Red Sea marine sponge *Lamellodysidea herbacea*. Tetrahedron 61, 955–963. https://doi.org/10.1016/j.tet.2004.11.011.

Sheldrick, G.M., 2008. A short history of SHELX. Acta Crystallogr. Sect. A: Foundations of Crystallography. 64, 112–122. https://doi.org/10.1107/S0108767307043930.
Sheldrick, G.M., 2015a. Shelxt – integrated space-group and crystal structure determination. Acta Cryst. A71, 3–8. https://doi.org/10.1107/S2053273314026370.
Sheldrick, G.M., 2015b. Crystal structure refinement with SHELXL. Acta Cryst C71, 3–8. https://doi.org/10.1107/S2053229614024218.
Sipkema, D., Franssen, M.C., Osinga, R., Tramper, J., Wijffels, R.H., 2005. Marine sponges as pharmacy. Mar. Biotechnol. 7, 142–162. https://doi.org/10.1007/s10126-004-0405-5.
Spek, A.L., 2009. Structure validation in chemical crystallography. Acta Cryst D65, 148–155. https://doi.org/10.1107/S090744490804362X.